Exact distribution of the vesicle burst size in synaptic transmission

Krishna Rijal[a], Nicolas I.C. Müller[b], Eckhard Friauf[b], Abhyudai Singh[c], Ashok Prasad[d,1], and Dibyendu Das[a,1]

[a]Department of Physics, Indian Institute of Technology Bombay, Powai, Mumbai 400076, India
[b]Animal Physiology Group, Department of Biology, University of Kaiserslautern, Kaiserslautern, Germany
[c]Departments of Electrical and Computer Engineering, Biomedical Engineering and Mathematical Sciences, University of Delaware, Newark, DE 19716, USA
[d]Department of Chemical and Biological Engineering, Colorado State University, Fort Collins, Colorado, USA
[1]To whom correspondence should be addressed: dibyendu@phy.iitb.ac.in; ashok.prasad@colostate.edu

December 28, 2022

Abstract

The transfer of electro-chemical signals from the pre-synaptic to the post-synaptic terminal of a neuronal or neuro-muscular synapse is the basic building block of neuronal communication. When triggered by an action potential the pre-synaptic terminal releases neurotransmitters in the synaptic cleft through vesicle fusion. The number of vesicles that fuse, i.e., the burst size, is stochastic, and widely assumed to be binomially distributed. However, the burst size depends on the number of release-ready vesicles, a random variable that depends upon a stochastic replenishment process, as well as stochastic inter-spike intervals of action potentials. The burst size distribution suitably averaged over these two stochastic processes was not known in the literature. Here we analytically obtain the exact probability distribution of the number of vesicles released in the synaptic cleft, in the steady state reached during stimulation by a spike train of action potentials. We show that this distribution is binomial, with modified parameters, only when stimulated by constant frequency signals. Other forms of input, e.g. Poisson-distributed action potentials, lead to distributions that are non-binomial. The general formula valid for arbitrary distributions of the input inter-spike interval, may be employed to study neuronal transmission under diverse experimental conditions. We corroborate our theoretical predictions through comparison with the burst size distributions obtained from electrophysiological recordings from MNTB-LSO synapses of juvenile mice. We also confirm our theoretically predicted frequency dependence of mean burst size by comparing with experimental data from hippocampal and auditory neurons.

Introduction

The human brain is arguably the most complex natural object in the known universe. Its complexity, as well as its capabilities, are a product of its roughly 10^{11} [1] neurons that make approximately 10^{15} connections [2] with each other. The majority of these connections are chemical synapses, where a pre-synaptic neuron communicates with a post-synaptic neuron through neurotransmitter release in a very narrow synaptic cleft (Fig. 1a). Neurotransmitter release takes place by the fusion of neurotransmitter-containing lipid vesicles with the pre-synaptic plasma membrane at the synaptic cleft, thereby releasing their cargo into the cleft (Fig. 1a). Synaptic Vesicle (SV) fusion is controlled by calcium dynamics and is initiated by an action potential (AP) in the pre-synaptic neuron, Neurotransmitter release may cause either an excitatory or inhibitory signal at the post-synaptic terminal, that could result in an action potential or the suppression of one [3]. Thus, SV release from pre-synaptic terminals is a fundamental feature of all information processing in the brain.

Decades of study since Castillo and Katz [4] first proposed the quantal theory of neurotransmitter release have revealed the basic characteristics of the process. The swelling or bouton in the pre-synaptic neuron that constitutes the pre-synaptic terminal contains vesicle-rich active zones (AZ) proximal to the plasma membrane. The AZ regions are surrounded by a larger vesicle-rich area, as well as mitochondria that supply energy and help regulate calcium dynamics, and dense actin filaments involved

in vesicle transport and recycling [5, 6]. Detailed micro-structural and electrophysiological studies have led to a consensus on a vesicle pool model of neurotransmitter release at a descriptive level [6–8]. According to this model, SVs can be divided into two or three pools. The smallest pool is the readily-releasable pool (RRP) situated in the AZ, that is released immediately after stimulation. The remaining pools are the Recycling pool (RP) and the Resting pool [7] (also named reserve pool in [6]). The sizes of the pool vary widely between different types of neurons and different species, and also within individual boutons of a single neuron [7]. Arrival of an AP at the pre-synaptic terminal leads to fusion of vesicles from the RRP with the plasma membrane and release of the neurotransmitter cargo in the synaptic cleft. As the RRP is depleted, vesicles from the RP are mobilized to replenish the docking sites in the AZ, and vesicle recycling also kicks in. With continual stimulation the vesicles from the Resting pool may get mobilized, however this depends upon the type of neuron. In human hippocampal neurons, for example, the Resting pool seems to be rarely activated [6].

Thus, SV fusion in most neurons is well described by a two-pool model (Fig. 1a) and a two-step process. Initially, each AP releases a fraction of the docked vesicles constituting the RRP, leading to a decline in the average number of vesicles released over time. With sustained stimulation the RRP starts to be replenished from the recycling pool and ultimately, a balance between SV fusion and replenishment leads to the development of a steady state, so long as the rate of stimulus does not exceed the maximum capacity for replenishment [7,9]. The vesicle release process is therefore intrinsically stochastic and is one of the important sources of noise in the nervous system [10]. Vesicle release noise affects the information transfer from a pre-synaptic neuron to a postsynaptic neuron, and it has been argued that it may sometimes enhance information processing at synapses [11, 12].

Though much of the earlier analysis on theoretical modeling of synaptic transmission was carried out assuming a deterministic process [13–15], there is a significant literature studying the process using a probabilistic approach [16–22]. Empirical observations had shown that the Binomial distribution was a good fit to the statistics of quantal release as far back as 1975, and this has been the basis of the majority of fluctuation analysis [12, 16, 20, 22–27]. Limitations of the binomial assumption due to biological complexities was recognized (reviewed in Ref. [8]). But it has generally been assumed that the basic model of neurotransmitter release follows a binomial distribution of the number of released vesicles b (here also called burst size) [12, 20–22, 28–30], namely $\beta(n_-, p_r, b) = \binom{n_-}{b} p_r^b (1-p_r)^{n_- - b}$, where probability of release is p_r. Since the replenishment process is itself stochastic, the number of docked vesicles n_- just prior to a burst is random. Approximate theories in the literature took this as some adhoc fixed number or replaced it by its mean value $\langle n_- \rangle$, in the steady state [20–22, 28, 29, 31, 32]. Moreover some treatments concluded that the distribution is Poisson or Gamma [12, 33].

In this paper we show that retaining a binomial formula in the steady state by using an *ad hoc* approximation of the number of docked vesicles n_-, is far from being adequate. A more careful approach leads to a revision of the binomial form itself after accounting for the stochasticity in n_- arising from various sources. Firstly the

replenishment process through which the docked vesicle number n varies, is described by a probability distribution $p(n,t)$. Secondly the replenishment process is terminated by the appearance of an AP potential at $t = t_s$ when we have $n = n_-$, and this time interval t_s may also be stochastic in general and drawn from a distribution $g(t_s)$ (see Fig. 1b). We show analytically exactly, that the original binomial distribution $\beta(n_-, p_r, b)$ averaged over the mentioned sources of stochasticity of n_- becomes functionally entirely distinct for every $g(t_s)$. For the commonly studied case where $g(t_s)$ represents action potentials occurring at fixed time intervals, the revised distribution continues to be a binomial but with new parameters, i.e. $\beta(M, p_{rb}, b)$ — where p_r is replaced by a p_{rb} (which depends on the time gaps of AP apart from p_r), and M is the maximum number of docked vesicles. For AP following a Poisson process, that is $g(t_s)$ being exponential, the derived distribution is not binomial. The analytical formula that we provide is usable for any functional form of $g(t_s)$ that the experimental AP spike train may have, and generically, we claim that non-binomial vesicle burst size distributions are expected.

The analysis presented here is restricted to the steady-state response of the pre-synaptic terminal. We do not include any of the processes involved in the transient or initial response to APs by previously resting synapses such as short-term depression (shown in Fig. 1b as the decline in b immediately after the commencement of the signal), or any other forms of short-term plasticity. We assume therefore that calcium dynamics, which is required for vesicle fusion, has also reached a steady state, and do not consider it explicitly. We also do not explicitly consider the process of vesicle priming [34] but assume a simple model in which all processes including transport and priming that prepares vesicles for fusion can be incorporated into a rate k (Fig. 1a). In steady state the parameters p_r and k are constants. These assumptions are consistent with experimental data and previous models [12,20–22,28,30,35]. Finally, we also do not consider processes in the post-synaptic terminal after neurotransmitter release.

Results

A stochastic model of vesicle release triggered by action potential

A schematic diagram of a chemical synapse is shown in Fig. 1a, with the vesicle-rich pre-synaptic terminal on the left and the post-synaptic terminal with neurotransmitter receptors on the right. The cartoon shows only a few vesicles but the actual number in the pre-synaptic terminal are in the hundreds [36,37]. In the pre-synaptic terminal, SVs packed with neurotransmitters attach to docking sites. The arrival of an AP triggers the stochastic fusion of a few SVs with the pre-synaptic membrane followed by neurotransmitter release. We assume that there are a maximum number M of available docking sites, and that docking sites are refilled from the vesicle pool at a rate proportional to the number of empty sites, i.e., a rate equal to $k(M - n)$, where n is the number of already docked vesicles and k is the docking rate per empty

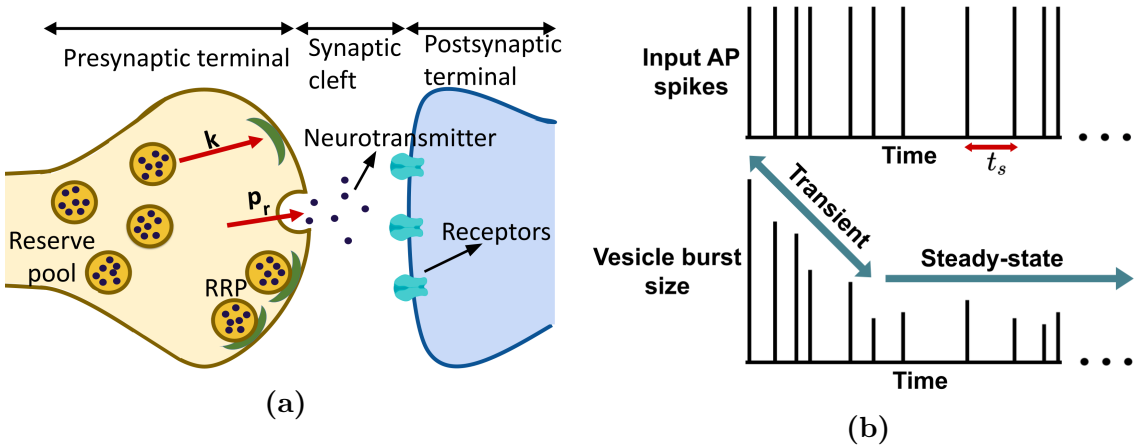

Figure 1: A schematic of the synapse and synaptic communication data. (a) Schematic picture of a chemical synapse. On the left is the pre-synaptic terminal or bouton and on the right is the post-synaptic terminal, with the synaptic cleft in between. The pre-synaptic terminal contains a pool of docked vesicles (RRP) and another reserve pool of vesicles that can occupy empty docked sites after vesicle fusion. The rate of docking k and the fusion and release probability p_r of vesicles are shown. The post-synaptic terminal has receptors for the neurotransmitters released from the fused vesicles. (b) Synaptic communication. The illustration shows an input spike train with random intervals t_s, and the output vesicle burst size with initial transient and eventual steady-state regions.

site [20, 22]. We consider experimentally relevant scenarios (like in Ref. [35]) where a spike train arrives at the pre-synaptic neuron. In this study we consider the general possibility that the time intervals t_s between two consecutive spikes of the input AP may be random, following a distribution $g(t_s)$. Experimentally often fixed frequency oscillatory input AP are used with constant $t_s = T$ [20, 21, 30, 35], which would correspond to $g(t_s) = \delta(t_s - T)$. The number b of SVs that fuse after the arrival of an AP is a stochastic variable, which we refer to as the vesicle *burst size*. We assume following [12, 20, 21, 28, 30], that the burst size b after an AP follows a binomial distribution $\beta(n_-, p_r, b) = \binom{n_-}{b} p_r^b (1 - p_r)^{n_- - b}$, where p_r is the probability of release (in the steady state) and n_- is the instantaneously docked vesicle number when the AP arrives.

We note that the burst size b is stochastic not just because it is binomially distributed, but because the number of docked vesicles n_- which form its source is itself stochastic. As we discussed above, the ready to release docked vesicle number n grows stochastically with time, and at random intervals t_s when an AP appears, $n = n_-$ suddenly become $n = n_- - b$. Thus in the steady state, the exact distribution of b may be obtained by averaging the binomial over the stochastic n_-, which leads to a revised distribution as we would see below.

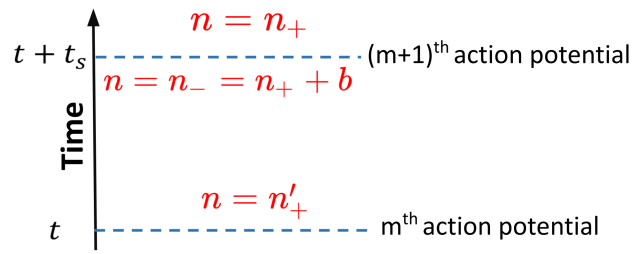

Figure 2: Model variables. Schematic showing the variables we used to describe the time evolution of the number n of the vesicles inside the pre-synaptic neuron, from the value n'_+ after an action potential to n_- just prior to the next action potential after time t_s and then its sudden reduction to n_+ after a burst of size b.

The burst size distribution $B^{ss}(b)$ in the steady state

In Fig. 2, the number variation of vesicles in the pre-synaptic neuron is shown schematically. Starting with $n = n'_+$ after an AP, the number grows to $n = n_- = n_+ + b$ in time t_s, at which the appearance of the next AP leads to the fusion of b vesicles, resulting in a sudden decrease of n from $n_+ + b$ to n_+. Before the arrival of APs in the pre-synaptic terminal, the instantaneous number of docked vesicles n_- may be assumed to be at its maximum value, M, and the burst size b is thus expected to be the largest. With the continuation of the stimulus, the average number of n_- gradually decreases to a steady-state level given by a balance between the vesicle release and replenishment process. In this long-time steady-state limit, our goal is to obtain an explicit expression for the size distribution $B^{ss}(b)$ of b averaged over the stochastic vesicle number n_-, as follows:

$$B^{ss}(b) = \sum_{n_-=0}^{M} \beta(n_-, p_r, b) P_-^{ss}(n_-). \tag{1}$$

To calculate $B^{ss}(b)$ we need to first obtain $P_-^{ss}(n_-)$, the steady-state probability distribution of having $n = n_-$ docked vesicles just before an action potential. As mentioned previously, n_- and hence $P_-^{ss}(n_-)$ is regulated by the random processes of growth of n and the appearance of AP at a random t_s. To study the growth of n, we introduce the time-dependent conditional probability $p(n, t|n'_+)$, of having n number of docked vesicles at time t, given n'_+ docked vesicles at $t = 0$, i.e. just after the previous action potential (see Fig. 2). In terms of this conditional probability, the distribution $P_-^{ss}(n_-)$ in Eq. (1) is given by averaging $p(n, t_s|n'_+)$ over both the inter-spike interval t_s as well as the initial number n'_+. Note that we are using primed variables to distinguish variables at the *previous* AP from those at the current AP.

$$P_-^{ss}(n_-) = \sum_{n'_+} \int_0^\infty p\left(n_-, t_s \mid n'_+\right) P_+^{ss}(n'_+) g(t_s) dt_s, \tag{2}$$

where $P_+^{ss}(n'_+)$ is the steady-state probability distribution of having $n = n'_+$ just after an action potential. Since the distribution of inter-spike intervals is given

experimentally, we need to calculate the other two distributions inside the integral on the right.

The conditional distribution $p(n,t|n'_+)$ of n between two successive action potentials describes the time-dependent replenishment process, and thus satisfies the corresponding Master equation [38],

$$\frac{\partial p(n,t|n'_+)}{\partial t} = k\left(M-(n-1)\right)p(n-1,t|n'_+) - k(M-n)p(n,t|n'_+). \tag{3}$$

This equation can be solved using the generating function $F(q,t|n'_+) = \sum_n q^n p(n,t|n'_+)$ (see Appendix 1 for the details), and we obtain the solution as,

$$p(n,t|n'_+) = \binom{M-n'_+}{n-n'_+}\left(1-e^{-kt}\right)^{n-n'_+} e^{-[k(M-n)]t}. \tag{4}$$

We next need to calculate $P_+^{ss}(n_+)$, the steady-state probability distribution of having n_+ docked vesicles *immediately after* the vesicle release following an action potential. This is non-trivial since $n_+ = n_- - b$, and since n_- depends upon the n'_+ of the previous interval, the result for any interval depends upon the results of the previous interval. By explicitly summing up over the history of the process in the steady state (see Appendix 2 for the derivation), we are able to obtain a self-consistent equation for $P_+^{ss}(n_+)$:

$$P_+^{ss}(n_+) = \sum_{n'_+,b}\int_0^\infty dt_s g(t_s)p(n_+ + b, t_s|n'_+)\beta(n_+ + b, p_r, b)P_+^{ss}(n'_+). \tag{5}$$

Eq. (5) contains the unknown $P_+^{ss}(n_+)$ on both sides. Other quantities are known, including $p(n_+ + b, t_s|n'_+)$ (from Eq. (4)). In a difficult and lengthy calculation (see details in Appendix 3) we show that the corresponding generation function to the above distribution, namely $F_+(q) = \sum_{n_+=0}^\infty q^{n_+}P_+^{ss}(n_+)$ can be obtained using the knowledge of $F(q,t|n'_+)$, the generating function for $p(n,t|n'_+)$) mentioned above. This generating function leads us to the other two relevant generating functions $F_-(q) = \sum_{n_-=0}^\infty q^{n_-}P_-^{ss}(n_-)$ and $F_b(q) = \sum_{b=0}^\infty q^b B^{ss}(b)$ corresponding to the distributions $P_-^{ss}(n_-)$ and $B^{ss}(b)$. Since the three stochastic variables, $n_-, n_+,$ and b are related to each other (namely $n_+ = n_- - b$), the generating functions must be too, and we can show that (see details in Appendix 4) they are related as:

$$F_-(q) = F_+\left(\frac{q-p_r}{1-p_r}\right) \text{ and } F_b(q) = F_+\left(\frac{p_r(q-1)}{1-p_r}+1\right). \tag{6}$$

From the knowledge of $F_b(q)$, we may finally obtain the desired distribution of burst size $B^{ss}(b)$ (see Appendix 4) using the standard relationship $B^{ss}(b) = \frac{1}{b!}\frac{\partial^b F_b(q)}{\partial q^b}\Big|_{q=0}$ [38]:

$$B^{ss}(b) = \sum_{n=0}^{\infty} \binom{n}{b} (-1)^{n-b} \binom{M}{n} \frac{p_r^n}{1-(1-p_r)^n L_n} \Bigg[\phi_{n,0} + \sum_{\{S_{(n-1)}\}} \frac{(1-p_r)^{\sum_i m_i} \phi_{n,m_z} \phi_{m_z,m_{z-1}} \cdots \phi_{m_1,0}}{\prod_i (1-(1-p_r)^{m_i} L_{m_i})} \Bigg], \tag{7}$$

where,

$$\begin{aligned} \phi_{n,m} =& \binom{n}{m} \int_0^\infty dt_s g(t_s) e^{-nkt_s} (e^{kt_s}-1)^{n-m}, \\ L_n =& \phi_{n,n} = \int_0^\infty dt_s g(t_s) e^{-nkt_s}. \end{aligned} \tag{8}$$

Here $\{S_{(n-1)}\}$ denotes the set of all the subsets $S_{(n-1)} = \{m_i\} = (m_z, m_{z-1}, \cdots, m_1)$ with $m_i \in (1, 2, \cdots, n-1)$ such that $m_z > m_{z-1} > \cdots > m_1$. Although the upper limit of the sum is shown up to ∞, due to the combinatorial factor $\binom{M}{n}$, n never exceeds M.

Eq. (7) for $B^{ss}(b)$ allows calculation of the exact burst size distribution given any experimentally or theoretically determined inter-spike probability distribution $g(t_s)$. Note that for an arbitrary $g(t_s)$ there is no reason to expect that $B^{ss}(b)$ in Eq. (7) would reduce to a binomial distribution.

We now calculate $B^{ss}(b)$ explicitly for two special cases of a fixed time interval (i.e. constant frequency), as well as for Poissonian time intervals between successive action potentials.

Fixed frequency spike trains

When t_s *is deterministic*, we have an AP spike train at a fixed frequency $f = 1/T$, and $g(t_s) = \delta(t_s - T)$. When we substitute this in Eq. (7), we find (see details in Appendix 5(a)) that the expression for $B^{ss}(b)$ reduces to a binomial distribution:

$$B^{ss}(b) = \beta(M, p_{rb}, b) \tag{9}$$

$$\text{where } p_{rb} = \frac{(1-e^{-kT})p_r}{1-(1-p_r)e^{-kT}} \tag{10}$$

Thus the steady state burst size distribution corresponding to a deterministic train of APs is indeed a binomial. However, Eq. (9) *is not equivalent to the approximate binomial often assumed in the literature, namely* $\beta(\langle n_- \rangle, p_r, b)$. In contrast the exact distribution has the parameters M and a modified release probability p_{rb} given by Eq. (10), which depends in the interval T and growth rate k apart from p_r. In fact we may calculate exactly $\langle n_- \rangle = M p_{rb}/p_r$ now (see Appendix 5(a)), and use that to compute the approximate binomial formula $\beta(\langle n_- \rangle, p_r, b)$. We note that the

result of the heuristic model presented in Ref. [20] is equivalent to Eq. (9) for this special case of fixed frequency APs.

Since Kinetic Monte Carlo simulations of the full stochastic growth and vesicle release process is expected to give a numerically accurate answer for the steady state distribution of the burst size, we proceed to compare it with the exact distribution. In Fig. 3, we see that the exact binomial distribution of $B^{ss}(b)$ (Eq. (9)) matches perfectly the data from Kinetic Monte Carlo (KMC) simulations of this process (see the red symbols), while the approximate binomial $\beta(\langle n_- \rangle, p_r, b)$ deviates significantly. This validates the predicted difference between the exact and approximate binomial expressions.

The mean and coefficient of variation of the exact binomial distribution Eq. (9) are,

$$\langle b \rangle = M p_{rb} \quad \text{and} \quad CV^2 = \frac{(1 - p_{rb})}{M p_{rb}}, \tag{11}$$

We note that though the mean of the approximate binomial is $\langle n_- \rangle p_r = M p_{rb}$ (same as the exact binomial), its $CV^2 = \frac{(1-p_r)}{M p_{rb}}$ is clearly different from the exact CV^2 appearing in Eq. (11).

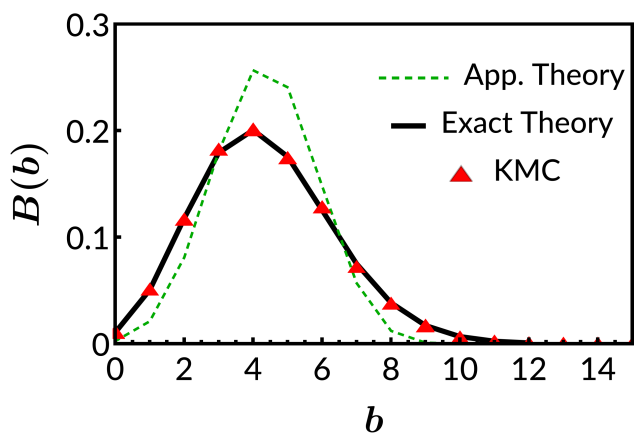

Figure 3: Burst size distribution under fixed AP arrival times. The exact (thick line) and approximate (dashed line) Binomial distributions (see text) of $B^{ss}(b)$ for the case of deterministic intervals T of AP are plotted. The data from Kinetic Monte Carlo simulations are shown in red symbols. The values of the parameters used are $M = 50$, $p_r = 0.5$, $k = 2$ sec^{-1} and $f = 1/T = 20$ Hz.

Poissonian spike trains

When the *AP train is a Poisson process*, the inter-spike intervals are exponentially distributed, $g(t_s) = f_0 e^{-f_0 t_s}$. We can substitute this expression in Eqs. (7) and (8) to obtain (details in Appendix 5(b)) the following expression for the steady state

burst size distribution:

$$B^{ss}(b) = \sum_{n=0}^{\infty}(-1)^{n-b}\binom{n}{b}\binom{M}{n}\frac{n!(kp_r)^n}{\prod_{i=1}^{n}(f_0 + ki - (1-p_r)^i f_0)}. \tag{12}$$

Note that this distribution is no longer a binomial. Thus even in one of the simplest cases of a stochastic $g(t_s)$, proper averaging over the sources which make n_- stochastic lead to a vesicle burst size distribution that is non-binomial. It is instructive to ask whether the binomial distribution for fixed time intervals derived in Eq. (9) above may be used as an approximation for the Poisson case — one may think that roughly the inverse rate $1/f_0$ may be equated to a constant interval T. The fact that this does not work is shown in Fig. 4 — while the numerically accurate Kinetic Monte Carlo data matches perfectly with the exact $B^{ss}(b)$ from Eq. (12), the binomial formula (Eq. (9)) with $T = 1/f_0$ differs significantly.

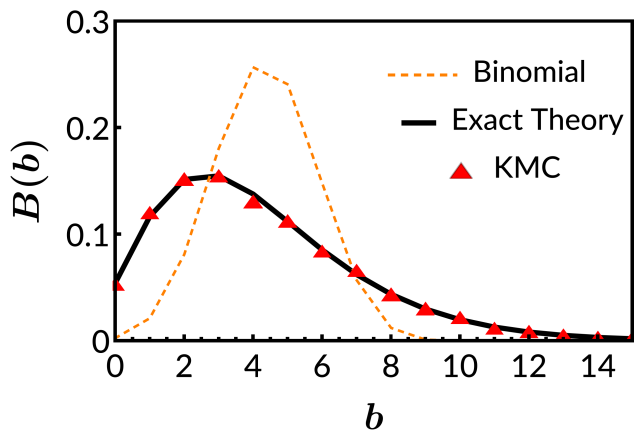

Figure 4: Burst size distribution under exponentially distributed AP arrival times. The exact distribution $B^{ss}(b)$ for exponentially distributed AP intervals from Eq. (12) is shown as a solid line, and the Kinetic Monte Carlo simulation data are shown in red symbols. The Binomial distribution of Eq. (9) with $T \to 1/f_0$, shown by a dashed line, is far from the correct curves. The parameter values are $M = 50$, $p_r = 0.5$, $k = 2$ sec^{-1} and $f_0 = 20$ Hz.

Distribution of experimentally obtained burst sizes and comparison with theory

To validate the predictions of our model we performed electrophysiological experiments, which are described in the Materials and methods section. The comparison between theory and experiment is done in Fig. 5. In Figs. 5a and 5b, for neuron-1 (left) and neuron-2 (right) respectively, we plot the time-varying fluctuating burst sizes for a single tetanic burst (in blue), as well as the mean burst size over 20 repeats (in red). In both neurons the mean burst size reaches a steady-state value beyond

0.8 s (see the yellow box). Considering burst sizes between times $0.8 - 1.0$ s over all the 20 histories, we obtained the normalised histogram of the experimental burst sizes – these are shown (in green) in Figs. 5c and 5d.

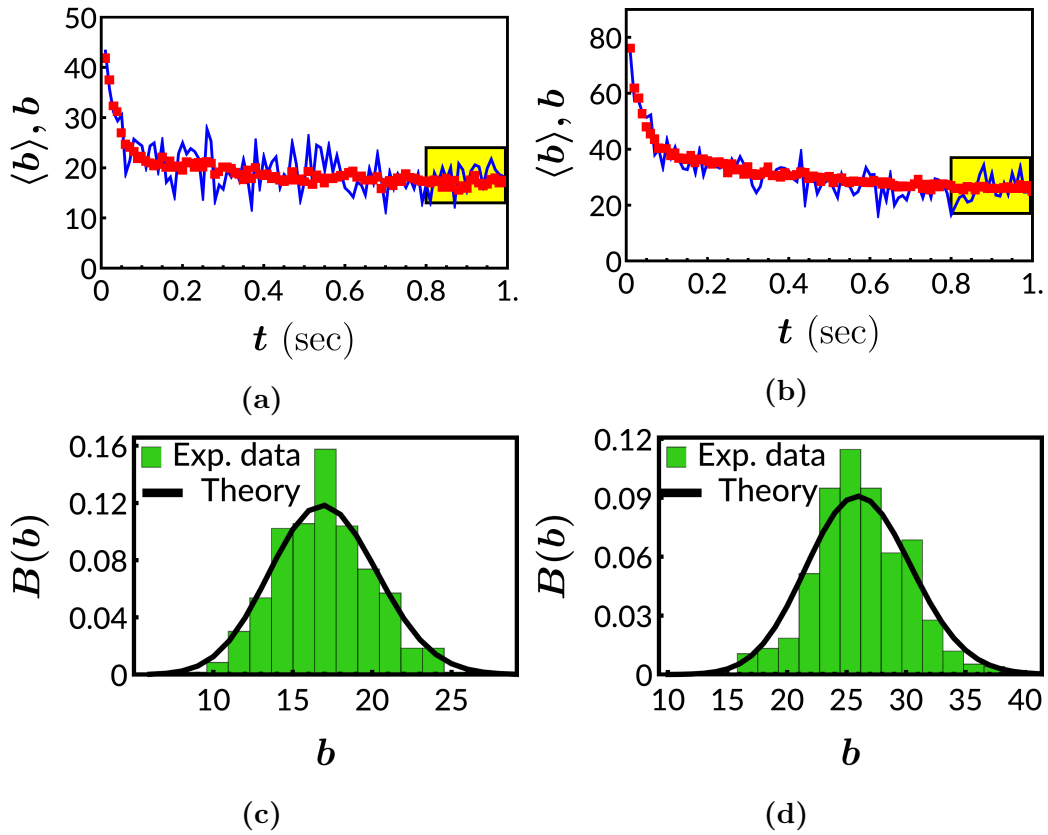

Figure 5: Comparing experimental distributions with predictions. The experimental mean burst size $\langle b \rangle$ is plotted (in red) against time, for (a) neuron-1 and (b) neuron-2. The blue curves represent one of the 20 experimental realizations of the burst size. The yellow box shows the part of data we considered to be in the steady state for plotting the experimental histograms of burst size in (c) and (d) (in green). In (c) and (d), the parameter values used for the exact theoretical distributions (black curves) for neuron-1 are $M = 50$ and $p_{rb} = 0.345$ and for the neuron-2 are $M = 98$ and $p_{rb} = 0.266$.

To compare the experimental data with the exact distribution Eq. (9), we first needed to estimate the parameters M and p_{rb} from experiments. We know that after the first AP (at 0 sec), the burst size b_0 follows a binomial distribution $\beta(M, p_{r0}, b_0)$, with a mean Mp_{r0} and variance $Mp_{r0}(1-p_{r0})$. From the 20 experimental histories we obtained the mean and variance of b_0 and using the theoretical formulas, obtained M by eliminating p_{r0}. Next we equate the experimental mean burst size (corresponding to the data in Figs. 5c and 5d) in the steady state, to the theoretical mean $\langle b \rangle = Mp_{rb}$ (Eq. (11)), and determine p_{rb}. With these parameters, we plot the exact distribution Eq. (9) and they match quite well to the experimental data in Figs. 5c and 5d (black curves). Note that without any fitting to match the noise in b the experimental and

theoretical CV^2 automatically turn out quite close. For neuron-1 the theory predicts 0.039 vs the experimental value of 0.032 while for neuron-2 the values are 0.028 (theory) vs 0.022 (experiment). The steady state values of p_r, k and T were not separately necessary to make the theory-experiment comparison, as they combine to give a single parameter p_{rb} which is sufficient.

Frequency dependence of mean burst size in the steady state – comparing theory to experiments

For a spike train at fixed time intervals T, the parameter p_{rb} (Eq. (10)) associated with the binomial and hence the mean burst size $\langle b \rangle = Mp_{rb}$ (Eq. (11)) follow a certain dependence on the frequency of stimulation $f = 1/T$. Experimental data for $\langle b \rangle$ as a function of f is available as published results in Ref. [35] for three different synapse types – two hippocampal (CA3 - CA1 and EC - DG) and one auditory (MNTB - LSO). The evoked postsynaptic currents were converted to $\langle b \rangle$ using appropriate quantal sizes. For each of the neurons, the values of p_r and the maximum vesicle docking rates kM are experimentally known [35]. Since we do not know the values of M and k separately, we do a one parameter fit with varying k to get the least square difference between the theoretical and experimental curves of $\langle b \rangle$ versus f. The best fit values of the parameter k and M thus obtained for the three neurons are provided in the caption of Fig. 6, and plots of the theoretical $\langle b \rangle$ (solid lines) are shown against the experimental values as a function of f. The extent of match demonstrates the usefulness of the exact formula (Eqs. (10,11)) for the frequency dependence of the mean burst size in the steady state.

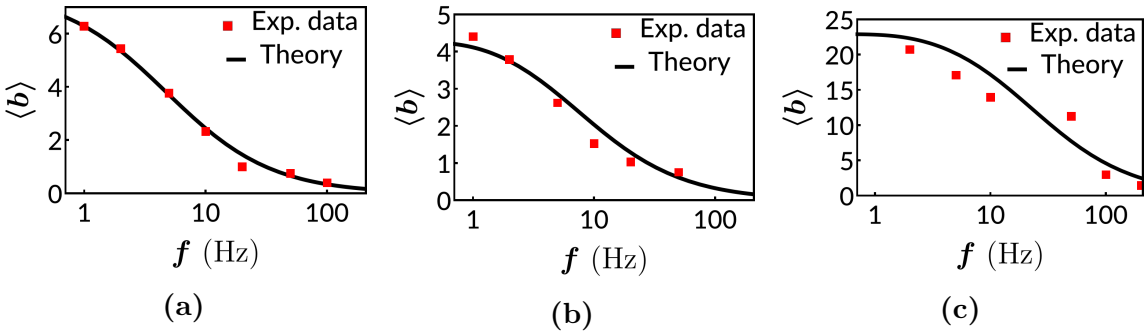

Figure 6: Comparing experimental frequency dependence of the mean burst size with model fits. The frequency dependence of the theoretical mean burst size is matched with the experimental values, for the neurons (a) CA3-CA1 (b) EC-DG and (c) MNTB-LSO. The experimental data was extracted from Ref. [35]. The theoretical curves were calculated using the parameter values obtained from the data provided in [35], followed by a one-parameter fit. The parameters are as follows: (a) $M = 688$, $p_r = 0.011$, $k = 0.0523$ sec^{-1} (b) $M = 17$, $p_r = 0.251$, $k = 2.058$ sec^{-1} (c) $M = 147$, $p_r = 0.156$, $k = 3.816$ sec^{-1}

Discussion

We make three basic biological assumptions in our work here, in line with much of the theoretical literature. (i) Our results apply when the burst size distribution has reached a steady state, and we do not consider the dynamics during the period of short-term plasticity before a steady state is achieved, shown by the region where $\langle b \rangle$ decays in Figs. 5a and 5b. (ii) We assume that the rate of replenishment is proportional to the number of empty docking sites. We do not therefore consider complexities in the replenishment process, for eg. pre-synaptic homeostasis [34, 42–45]. Many of these processes are compatible with the assumption of an approximately constant rate of replenishment, k, and our model is appropriate under this condition. (iii) Along with much of the literature, our model also assumes that the release probabilities of the vesicles, p_r is a constant during steady-state signaling at the pre-synaptic terminal. Recent advancements in the ultrastructural analysis of the neurons have suggested however that the release probabilities may be spatially heterogeneous [46, 47], which we do not consider in this work.

Incorporation of these additional complexities into a stochastic model of vesicle release is certainly possible in theory, but is likely to be a harder problem than the model solved here. However as our paper shows, a careful accounting of coupled stochastic processes is necessary to obtain theoretically robust results. For steady-state processes in particular, this involves proper averaging over stochastic trajectories. Since the quantal theory of neurotransmitter release, first proposed by Castillo et al. [4], it has been known that the vesicle release process is stochastic, and at least since 1975, it has often assumed that the statistics of vesicle release can be described by binomial distributions. For a model of quantal release with a probability of release p_r and n_- vesicles standing ready to be released, the statistics of vesicle release will be described by $\beta(n_-, p_r, b)$. However n_- itself is a stochastic variable that depends upon the processes of replenishing the RRP, as well as the time distribution of arrival-times, $g(t_s)$, of the action potential at the pre-synaptic terminal. The steady-state distribution of the burst-size therefore depends upon the proper averaging of these coupled stochastic processes.

In this paper we successfully perform this calculation, which yields a formula, Eq. (7), for the probability distribution of the burst sizes under the assumption of a reasonable kinetic replenishment model and arbitrary $g(t_s)$. Using this formula we show that when the arrival time of the APs are not fixed but follow the simplest random process, a Poisson process, the resultant burst size distribution deviates significantly from the binomial approximation. Eq. (12) is a strong prediction for the vesicle release distribution under exponentially varying arrival times, that would be very interesting to test.

Under the specific assumption of fixed arrival times of the APs, we find that Eq. (7) reduces to the binomial distribution given by Eq. (9). While this is in qualitative agreement with experiments performed under these conditions, it has typically been assumed previously that the binomial probability parameter of these empirical distributions is the same as the intrinsic probability of release from the post-synaptic terminal, p_r, and the size parameter is equivalent to the average size

of the RRP, $\langle n_- \rangle$. Here we show by exact calculation that the relevant binomial parameter of the distribution is not p_r but a different parameter p_{rb}, given by Eq. (10), and the size parameter is M, not the average but the maximum size of the RRP.

More generally, Eq. (7) is a prediction for the statistics of quantal release when the inter-spike timing of AP trains obey any probability distribution $g(t_s)$. This is significant for neuronal transmission *in vivo* because neural information is believed to be transmitted through differences in spiking rates [3]. Our results should thus be extremely useful for studying synaptic transmission under more physiologically realistic conditions.

Materials and Methods

Details of the derivations for analytical results are described in Appendices 1, 2, 3, 4, 5, 6, and 7.

Here we describe the protocols that were followed in the electrophysiological experiments. We performed electrophysiological experiments in acute brainstem slices of juvenile mice (postnatal day 11) at MNTB-LSO synapses. These fast auditory synapses transfer inhibitory glycinergic information and can maintain reliable neurotransmission even during prolonged high-frequency stimulation [39, 40]. We refer the reader to the Methods section of Ref. [40] for details on the slice preparation and details of whole-cell patch-clamp recordings. The stimulation protocol consisted of repetitive tetanic AP bursts (100 Hz, 1 s) that were given 20 times. A 30-s rest period was introduced between repeats to allow for recovery from short-term depression. The number of fused SVs was determined as the ratio of the peak amplitude of evoked inhibitory postsynaptic currents (eIPSC) to the current produced by a single quantum (q) [pA/(pA/SV)]. Detailed information is available in Refs. [40, 41].

Acknowledgements

DD acknowledges SERB India (Grant No. MTR/2019/ 000341) for financial support. KR thanks IIT Bombay for Institute Ph.D. fellowship. AS acknowledges support by NIH/NIDCD grant R01DC019268.

Competing interests

The authors declare no competing interests.

References

[1] S. Herculano-Houzel, "The human brain in numbers: a linearly scaled-up primate brain," *Front Hum Neurosci*, vol. 3, p. 31, 2009.

[2] Y. Tang, J. R. Nyengaard, D. M. De Groot, and H. J. Gundersen, "Total regional and global number of synapses in the human brain neocortex," *Synapse*, vol. 41, no. 3, pp. 258–73, 2001.

[3] E. R. Kandel, J. Koester, S. Mack, and S. Siegelbaum, *Principles of neural science*. New York: McGraw Hill, sixth edition. ed., 2021.

[4] J. Del Castillo and B. Katz, "Quantal components of the end-plate potential," *The Journal of physiology*, vol. 124, no. 3, p. 560, 1954.

[5] V. N. Murthy and P. De Camilli, "Cell biology of the presynaptic terminal," *Annu Rev Neurosci*, vol. 26, pp. 701–28, 2003.

[6] S. O. Rizzoli and W. J. Betz, "Synaptic vesicle pools," *Nat Rev Neurosci*, vol. 6, no. 1, pp. 57–69, 2005.

[7] A. A. Alabi and R. W. Tsien, "Synaptic vesicle pools and dynamics," *Cold Spring Harb Perspect Biol*, vol. 4, no. 8, p. a013680, 2012.

[8] E. Neher, "Merits and limitations of vesicle pool models in view of heterogeneous populations of synaptic vesicles," *Neuron*, vol. 87, no. 6, pp. 1131–1142, 2015.

[9] S. Weis, R. Schneggenburger, and E. Neher, "Properties of a model of ca++-dependent vesicle pool dynamics and short term synaptic depression," *Biophysical journal*, vol. 77, no. 5, pp. 2418–2429, 1999.

[10] D. A. Rusakov, L. P. Savtchenko, and P. E. Latham, "Noisy synaptic conductance: Bug or a feature?," *Trends in Neurosciences*, vol. 43, no. 6, pp. 363–372, 2020.

[11] M. S. Goldman, "Enhancement of information transmission efficiency by synaptic failures," *Neural computation*, vol. 16, no. 6, pp. 1137–1162, 2004.

[12] C. Zhang and C. S. Peskin, "Improved signaling as a result of randomness in synaptic vesicle release," *Proceedings of the National Academy of Sciences*, vol. 112, no. 48, pp. 14954–14959, 2015.

[13] M. V. Tsodyks and H. Markram, "The neural code between neocortical pyramidal neurons depends on neurotransmitter release probability," *Proceedings of the national academy of sciences*, vol. 94, no. 2, pp. 719–723, 1997.

[14] J. S. Dittman and W. G. Regehr, "Calcium dependence and recovery kinetics of presynaptic depression at the climbing fiber to purkinje cell synapse," *Journal of Neuroscience*, vol. 18, no. 16, pp. 6147–6162, 1998.

[15] J. S. Dittman, A. C. Kreitzer, and W. G. Regehr, "Interplay between facilitation, depression, and residual calcium at three presynaptic terminals," *Journal of Neuroscience*, vol. 20, no. 4, pp. 1374–1385, 2000.

[16] E. M. McLachlan, "The statistics of transmitter release at chemical synapses," *Int Rev Physiol*, vol. 17, pp. 49–117, 1978.

[17] S. Redman, "Quantal analysis of synaptic potentials in neurons of the central nervous system.," *Physiological Reviews*, vol. 70, no. 1, pp. 165–198, 1990. PMID: 2404288.

[18] A. Arleo, T. Nieus, M. Bezzi, A. d'Errico, E. d'Angelo, and O. J.-M. Coenen, "How synaptic release probability shapes neuronal transmission: information-theoretic analysis in a cerebellar granule cell," *Neural computation*, vol. 22, no. 8, pp. 2031–2058, 2010.

[19] R. Rosenbaum, J. Rubin, and B. Doiron, "Short term synaptic depression imposes a frequency dependent filter on synaptic information transfer," *PLoS computational biology*, vol. 8, no. 6, p. e1002557, 2012.

[20] C. Pulido, F. F. Trigo, I. Llano, and A. Marty, "Vesicular release statistics and unitary postsynaptic current at single gabaergic synapses," *Neuron*, vol. 85, no. 1, pp. 159–172, 2015.

[21] G. Malagon, T. Miki, I. Llano, E. Neher, and A. Marty, "Counting vesicular release events reveals binomial release statistics at single glutamatergic synapses," *Journal of Neuroscience*, vol. 36, no. 14, pp. 4010–4025, 2016.

[22] Z. Vahdat, Z. Xu, and A. Singh, "Modeling and characterization of neuronal synapses using stochastic hybrid systems," in *2019 IEEE 58th Conference on Decision and Control (CDC)*, pp. 4729–4734, IEEE, 2019.

[23] M. D. Miyamoto, "Binomial analysis of quantal transmitter release at glycerol treated frog neuromuscular junctions," *J Physiol*, vol. 250, pp. 121–42, Aug 1975.

[24] R. Malinow and R. W. Tsien, "Presynaptic enhancement shown by whole-cell recordings of long-term potentiation in hippocampal slices," *Nature*, vol. 346, pp. 177–80, Jul 1990.

[25] S. S. Kelly and N. Robbins, "Statistics of neuromuscular transmitter release in young and old mouse muscle," *J Physiol*, vol. 385, pp. 507–16, Apr 1987.

[26] R. A. Silver, A. Momiyama, and S. G. Cull-Candy, "Locus of frequency-dependent depression identified with multiple-probability fluctuation analysis at rat climbing fibre-purkinje cell synapses," *The Journal of physiology*, vol. 510, no. 3, pp. 881–902, 1998.

[27] H. Taschenberger, V. Scheuss, and E. Neher, "Release kinetics, quantal parameters and their modulation during short-term depression at a developing synapse in the rat cns," *The Journal of physiology*, vol. 568, no. 2, pp. 513–537, 2005.

[28] E. Hanse and B. Gustafsson, "Paired-pulse plasticity at the single release site level: an experimental and computational study," *Journal of Neuroscience*, vol. 21, no. 21, pp. 8362–8369, 2001.

[29] C. Pulido and A. Marty, "Quantal fluctuations in central mammalian synapses: functional role of vesicular docking sites," *Physiological reviews*, vol. 97, no. 4, pp. 1403–1430, 2017.

[30] G. Malagon, T. Miki, V. Tran, L. C. Gomez, and A. Marty, "Incomplete vesicular docking limits synaptic strength under high release probability conditions," *Elife*, vol. 9, p. e52137, 2020.

[31] A. Brémaud, D. C. West, and A. M. Thomson, "Binomial parameters differ across neocortical layers and with different classes of connections in adult rat and cat neocortex," *Proceedings of the National Academy of Sciences*, vol. 104, no. 35, pp. 14134–14139, 2007.

[32] H. Wen, M. J. McGinley, G. Mandel, and P. Brehm, "Nonequivalent release sites govern synaptic depression," *Proceedings of the National Academy of Sciences*, vol. 113, no. 3, pp. E378–E386, 2016.

[33] A. D. Bird, M. J. Wall, and M. J. Richardson, "Bayesian inference of synaptic quantal parameters from correlated vesicle release," *Frontiers in computational neuroscience*, vol. 10, p. 116, 2016.

[34] J. S. Lee, W.-K. Ho, E. Neher, and S.-H. Lee, "Superpriming of synaptic vesicles after their recruitment to the readily releasable pool," *Proceedings of the National Academy of Sciences*, vol. 110, no. 37, pp. 15079–15084, 2013.

[35] E. G. Krächan, A. U. Fischer, J. Franke, and E. Friauf, "Synaptic reliability and temporal precision are achieved via high quantal content and effective replenishment: auditory brainstem versus hippocampus," *The Journal of Physiology*, vol. 595, no. 3, pp. 839–864, 2017.

[36] K. Ikeda and J. M. Bekkers, "Counting the number of releasable synaptic vesicles in a presynaptic terminal," *Proc Natl Acad Sci U S A*, vol. 106, no. 8, pp. 2945–50, 2009.

[37] B. G. Wilhelm, S. Mandad, S. Truckenbrodt, K. Kröhnert, C. Schäfer, B. Rammner, S. J. Koo, G. A. Claßen, M. Krauss, V. Haucke, H. Urlaub, and S. O. Rizzoli, "Composition of isolated synaptic boutons reveals the amounts of vesicle trafficking proteins," *Science*, vol. 344, no. 6187, pp. 1023–1028, 2014.

[38] C. W. Gardiner, *Handbook of stochastic methods*, vol. 3. springer Berlin, 1985.

[39] S. E. Brill, A. Maraslioglu, C. Kurz, F. Kramer, M. F. Fuhr, A. Singh, and E. Friauf, "Glycinergic transmission in the presence and absence of functional glyt2: Lessons from the auditory brainstem," *Front Synaptic Neurosci*, vol. 12, p. 560008, 2020.

[40] N. I. C. Müller, I. Paulussen, L. N. Hofmann, J. O. Fisch, A. Singh, and E. Friauf, "Development of synaptic fidelity and action potential robustness at an inhibitory sound localization circuit: effects of otoferlin-related deafness," *J Physiol*, vol. 600, no. 10, pp. 2461–2497, 2022.

[41] N. I. C. Müller, M. Sonntag, A. Maraslioglu, J. J. Hirtz, and E. Friauf, "Topographic map refinement and synaptic strengthening of a sound localization circuit require spontaneous peripheral activity," *The Journal of Physiology*, vol. 597, no. 22, pp. 5469–5493, 2019.

[42] G. W. Davis, "Homeostatic control of neural activity: From phenomenology to molecular design," *Annual Review of Neuroscience*, vol. 29, no. 1, pp. 307–323, 2006. PMID: 16776588.

[43] H. Taschenberger, A. Woehler, and E. Neher, "Superpriming of synaptic vesicles as a common basis for intersynapse variability and modulation of synaptic strength," *Proceedings of the National Academy of Sciences*, vol. 113, no. 31, pp. E4548–E4557, 2016.

[44] J. M. Ortega, O. Genc, and G. W. Davis, "Molecular mechanisms that stabilize short term synaptic plasticity during presynaptic homeostatic plasticity," *eLife*, vol. 7, p. e40385, nov 2018.

[45] B. O. Orr, R. D. Fetter, and G. W. Davis, "Activation and expansion of presynaptic signaling foci drives presynaptic homeostatic plasticity," *Neuron*, 2022.

[46] D. Keller, N. Babai, O. Kochubey, Y. Han, H. Markram, F. Schürmann, and R. Schneggenburger, "An exclusion zone for ca2+ channels around docked vesicles explains release control by multiple channels at a cns synapse," *PLoS computational biology*, vol. 11, no. 5, p. e1004253, 2015.

[47] Y. Nakamura, H. Harada, N. Kamasawa, K. Matsui, J. S. Rothman, R. Shigemoto, R. A. Silver, D. A. DiGregorio, and T. Takahashi, "Nanoscale distribution of presynaptic ca2+ channels and its impact on vesicular release during development," *Neuron*, vol. 85, no. 1, pp. 145–158, 2015.

Appendix 1

Probability distribution of docked vesicle number n between two consecutive action potentials

Let $p(n,t|n'_+)$ denote the probability distribution of the number n of docked (ready to release) vesicles at time t, starting from $n = n'_+$ at $t = 0$ (i.e. from the instant of the last action potential (AP)). Thus t denotes any time up to the next AP, i.e. $t < t_s$ where t_s is a time when the next AP arrives. In the interval t to $t+dt$, the number of docked vesicles may increase from $n-1$ to n with the probability $k(M-(n-1))dt$. Here k is the growth rate per empty docking sites, and M is maximum number of docking sites. Consequently, the master equation for the time evolution of $p(n,t|n'_+)$ between two successive APs is:

$$\frac{\partial p(n,t|n'_+)}{\partial t} = k\left(M-(n-1)\right)p(n-1,t|n'_+) - k(M-n)p(n,t|n'_+) \tag{13}$$

We define a generating function for the above probability distribution:

$$F(q,t|n'_+) = \sum_n q^n p(n,t|n'_+) \tag{14}$$

Here the limits of the above sum are $n'_+ \leq n \leq M$. Otherwise, we assume $p(n,t|n'_+) = 0$ if n'_+ falls outside this range. Multiplying Eq. (13) by $\sum_n q^n$ on both sides, we get a PDE for the generating function F:

$$\begin{aligned}\frac{\partial F}{\partial t} =& + kM\sum_n q^n p(n-1,t|n'_+) - k\sum_n q^n(n-1)p(n-1,t|n'_+)\\ &- kM\sum_n q^n p(n,t|n'_+) + k\sum_n q^n np(n,t|n'_+) = kMqF - kq^2\frac{\partial F}{\partial q} - kMF + kq\frac{\partial F}{\partial q}\end{aligned}$$

Rearranging the terms, we have,

$$\frac{\partial F}{\partial t} + kq(q-1)\frac{\partial F}{\partial q} = kM(q-1)F \tag{15}$$

We use the method of Lagrange characteristics to solve the Eq. (15). The result is:

$$F(q,t|n'_+) = q^M\left[1 - \frac{(q-1)}{q}e^{-kt}\right]^{M-n'_+} \tag{16}$$

We do binomial expansion of Eq. (16) to get

$$\begin{aligned}F =& q^{n'_+}\left[q(1-e^{-kt}) + e^{-kt}\right]^{M-n'_+}\\ =& \sum_{n=0}^{M-n'_+}\binom{M-n'_+}{n}\left[q^{n+n'_+}\left(1-e^{-kt}\right)^n\right]\left(e^{-kt}\right)^{M-n'_+-n}\end{aligned}$$

and relabelling $n + n'_+ \to n$ we get

$$F = \sum_{n=n'_+}^{M} \binom{M - n'_+}{n - n'_+} q^n \left(1 - e^{-kt}\right)^{n-n'_+} \left(e^{-kt}\right)^{M-n} \tag{17}$$

Next we can compare Eq. (17) with Eq. (14) to get the expression of $p(n, t|n'_+)$:

$$\boxed{p(n, t|n'_+) = \binom{M - n'_+}{n - n'_+} \left(1 - e^{-kt}\right)^{n-n'_+} e^{-[k(M-n)]t}} \tag{18}$$

for $n'_+ \leq n < \infty$. Note that for $n > M$, the probability goes to zero automatically in the above expression.

Appendix 2

Self-consistent equation for the vesicle burst size distribution $P_+^{ss}(n_+)$ in the steady state

Let us denote the time intervals between $(m-1)^{th}$ AP and m^{th} AP by t_{sm} and between the $(m-2)^{th}$ AP and $(m-1)^{th}$ AP by t_{sm-1}. We first relate the probability $P_+^m(n_{+,m}, t_{sm})$ of having $n_{+,m}$ number of docked vesicles after the mth AP, to the probability $P_+^{m-1}(n_{+,m-1}, t_{sm-1})$ of having $n_{+,m-1}$ number of vesicles just after the $(m-1)^{th}$ AP. To do so, we need to sum over all possible paths beginning at $n = n_{+,m-1}$ after the $(m-1)^{th}$ action potential and ending at $n = n_{+,m}$ after the mth AP. The sum involves the product of three probabilities due to a sequence of steps: (i) initial $P_+^{m-1}(n_{+,m-1}, t_{sm-1})$, then (ii) the probability $p(n_{+,m} + b, t_{sm}|n_{+,m-1})$ that $n_{+,m-1}$ rises to $n_{+,m} + b$ in time t_{sm}, and (iii) finally the probability that at t_{sm}, the number $n_{+,m} + b$ of docked vesicles suddenly reduce to $n_{+,m}$ due to the AP triggered vesicle release, with the associated burst size b being binomially distribution $\beta(n_{+,m} + b, p_r, b)$. After summing over all possible initial number $n_{+,m-1}$ and burst size b we have,

$$P_+^m(n_{+,m}, t_{sm}) = \sum_{n_{+,m-1},b} \beta(n_{+,m}+b, p_r, b) p(n_{+,m}+b, t_{sm}|n_{+,m-1}) P_+^{m-1}(n_{+,m-1}, t_{sm-1}) \tag{19}$$

We may follow the same procedure for $P_+^{m-1}(n_{+,m-1}, t_{sm-1})$ and so on, and build up a hierarchy of relations for any interval between two APs. The problem remains hard to solve as result for every interval depends on the history of the previous interval. We are particularly interested in the steady state attained after several APs appear, i.e. $m \gg 1$ and the output burst sizes statistically stabilise. In such a situation, we have a steady state probability distribution of vesicle number after any AP given by $P_+^{ss}(n_{+,m}) = \int_0^\infty dt_{sm-1} g(t_{sm-1}) P_+^{m-1}(n_{+,m-1}, t_{sm-1})$. The averaging over the distribution of time intervals t_{sm} remove the history dependence. Taking

average of Eq. (19) with respect to the normalised distributions $g(t_{sm})$ and $g(t_{sm-1})$ of t_{sm} and t_{sm-1} respectively, we have

$$\begin{aligned}
&\int_0^\infty \int_0^\infty dt_{sm} dt_{sm-1} g(t_{sm}) g(t_{sm-1}) P_+^m(n_{+,m}, t_{sm}) \\
&= \int_0^\infty \int_0^\infty dt_{sm} dt_{sm-1} g(t_{sm}) g(t_{sm-1}) \\
&\quad \times \sum_{n_{+,m-1},b} p(n_{+,m}+b, t_{sm}|n_{+,m-1}) \beta(n_{+,m}+b, p_r, b) P_+^{m-1}(n_{+,m-1}, t_{sm-1}) \\
&\Rightarrow \int_0^\infty dt_{sm} g(t_{sm}) P_+^m(n_{+,m}, t_{sm}) \\
&= \sum_{n_{+,m-1},b} \int_0^\infty dt_{sm} g(t_{sm}) p(n_{+,m}+b, t_{sm}|n_{+,m-1}) \beta(n_{+,m}+b, p_r, b) \\
&\quad \times \int_0^\infty dt_{sm-1} g(t_{sm-1}) P_+^{m-1}(n_{+,m-1}, t_{sm-1}) \qquad (20)
\end{aligned}$$

Finally dropping the subscripts m (in the steady state), and setting $t_s = t_{sm}$ and $n'_+ = n_{+,m-1}$, the Eq. (20) becomes

$$\boxed{P_+^{ss}(n_+) = \sum_{n'_+,b} \int_0^\infty dt_s g(t_s) p(n_+ + b, t_s|n'_+) \beta(n_+ + b, p_r, b) P_+^{ss}(n'_+)} \qquad (21)$$

Note that this is a self-consistent equation for the unknown $P_+^{ss}(n_+)$, when we know $g(t_s)$, $\beta(n_+ + b, p_r, b)$ and $p(n_+ + b, t_s|n'_+)$ (Eq. (18)). We analytically treat it in the next section.

Appendix 3

Generating function of the distribution $P_+^{ss}(n_+)$ in the steady state:

We define a generating function of $P_+^{ss}(n_+)$ as follows and solve it in this section:

$$F_+(q) = \sum_{n_+} q^{n_+} P_+^{ss}(n_+) \qquad (22)$$

In Eq. (21), the limits of the summation are $0 \le b \le M - n_+$ and $0 \le n'_+ \le n_+ + b$. Since anyways, $p(n_+ + b, t_s|n'_+) = 0$ outside the limits (see Eq. (18)), we may as well use the range $0 \le b, n'_+ \le \infty$. Multiplying Eq. (21) by q^{n_+} and summing over n_+ (with $0 \le n_+ \le \infty$), we have:

$$F_+(q) = \sum_{n'_+,b} \int_0^\infty dt_s g(t_s) \sum_{n_+} q^{n_+} p(n_+ + b, t_s|n'_+)\beta(n_+ + b, p_r, b) P_+^{ss}(n'_+) \tag{23}$$

We introduce a new variable $\tilde{n_+} = n_+ + b$ with $b \leq \tilde{n_+} \leq \infty$. Note that $\beta(\tilde{n_+}, p_r, b) = 0$ for $\tilde{n_+} < b$, so we may keep the range $0 \leq \tilde{n_+} \leq \infty$.

$$F_+(q) = \int_0^\infty dt_s g(t_s) \sum_{n'_+,b} \sum_{\tilde{n_+}} q^{\tilde{n_+}-b} p(\tilde{n_+}, t_s|n'_+)\beta(\tilde{n_+}, p_r, b) P_+^{ss}(n'_+) \tag{24}$$

Summing over b after substituting $\beta(\tilde{n_+}, p_r, b) = \binom{\tilde{n_+}}{b} p_r^b (1-p_r)^{\tilde{n_+}-b}$, we have

$$\begin{aligned} F_+(q) &= \int_0^\infty dt_s g(t_s) \sum_{n'_+} \sum_{\tilde{n_+}} \left(1 - p_r + \frac{p_r}{q}\right)^{\tilde{n_+}} q^{\tilde{n_+}} p(\tilde{n_+}, t_s|n'_+) P_+^{ss}(n'_+) \\ &= \int_0^\infty dt_s g(t_s) \sum_{n'_+} \sum_{\tilde{n_+}} (q - qp_r + p_r)^{\tilde{n_+}} \, p(\tilde{n_+}, t_s|n'_+) P_+^{ss}(n'_+) \end{aligned}$$

Doing summation over $\tilde{n_+}$ and using the definition of the generating function F (from Eq. (14)), we get

$$F_+(q) = \int_0^\infty dt_s g(t_s) \sum_{n'_+} F((q - qp_r + p_r), t_s|n'_+) P_+^{ss}(n'_+)$$

Defining $h(q) = (q - qp_r + p_r)$ and using Eq. (16) for the explicit form of function F:

$$\begin{aligned} F_+(q) &= \int_0^\infty dt_s g(t_s) \sum_{n'_+} h^M \left[1 - \frac{h-1}{h} e^{-kt_s}\right]^{M-n'_+} P_+^{ss}(n'_+) \\ &= \int_0^\infty dt_s g(t_s) \left[h - (h-1)e^{-kt_s}\right]^M \sum_{n'_+} \left(\frac{h}{h-(h-1)e^{-kt_s}}\right)^{n'_+} P_+^{ss}(n'_+) \\ &= \int_0^\infty dt_s g(t_s) \left[h - (h-1)e^{-kt_s}\right]^M F_+\left[\frac{h}{h-(h-1)e^{-kt_s}}\right] \\ &= \int_0^\infty dt_s g(t_s) \left[h(1-e^{-kt_s}) + e^{-kt_s}\right]^M F_+\left[\frac{h}{h(1-e^{-kt_s}) + e^{-kt_s}}\right] \end{aligned} \tag{25}$$

In the above we have used the definition of F_+ from Eq(22). In Eq. (25) we have a self-consistent integral equation for the function F_+ with two different arguments, and involving an integration over the inter-spike interval t_s. Clearly, it is difficult to solve the equation directly for $F_+(q)$. But as we show below, $F_+(q)$ may be obtained as a series expansion around $q = 1$, that is

$$F_+(q) = \sum_{n=0}^{\infty} \frac{(q-1)^n}{n!} F_+^{(n)}(1) \tag{26}$$

where the series coefficients $F_+^{(n)}(1) = \left.\frac{\partial^n F_+(q)}{\partial q^n}\right|_{q=1}$. The procedure of obtaining these coefficients are as follows.
Taking derivative with respect to q on both side of Eq. (25), we have

$$\begin{aligned}\frac{\partial F_+(q)}{\partial q} =& \frac{\partial h}{\partial q} \int_0^\infty dt_s g(t_s) \left(M \left[h(1-e^{-kt_s}) + e^{-kt_s}\right]^{M-1} (1-e^{-kt_s}) F_+ \left[\frac{h}{h(1-e^{-kt_s}) + e^{-kt_s}}\right] \right. \\ & \left. + \left[h(1-e^{-kt_s}) + e^{-kt_s}\right]^M \frac{\partial F_+[\ .\ ]}{\partial[\ .\ ]} \frac{e^{-kt_s}}{(h(1-e^{-kt_s}) + e^{-kt_s})^2} \right)\end{aligned} \tag{27}$$

where $[\ .\ ]$ is a short hand for $\left[\frac{h}{h(1-e^{-kt_s})+e^{-kt_s}}\right]$. Since $\frac{\partial h}{\partial q} = (1-p_r)$, $h(q)\big|_{q=1} = 1$, $[\ .\ ]\big|_{q=1} = 1$, $F_+(1) = 1$, and $\left.\frac{\partial F_+[\ .\ ]}{\partial[\ .\ ]}\right|_{q=1} = \left.\frac{\partial F_+(q)}{\partial q}\right|_{q=1}$, we have

$$\left.\frac{\partial F_+(q)}{\partial q}\right|_{q=1} = (1-p_r) \int_0^\infty dt_s g(t_s) \left(M(1-e^{-kt_s}) + \left.\frac{\partial F_+(q)}{\partial q}\right|_{q=1} e^{-kt_s} \right) \tag{28}$$

Defining the quantities $\psi_{n,m}$ and L_n as follows,

$$\begin{aligned}\psi_{n,m} =& \int_0^\infty dt_s g(t_s) e^{-nkt_s} (e^{kt_s} - 1)^{n-m} \\ L_n =& \psi_{n,n} = \int_0^\infty dt_s g(t_s) e^{-nkt_s}\end{aligned} \tag{29}$$

we have

$$F_+^{(1)}(1) = (1-p_r) \left(M\psi_{1,0} + L_1 F_+^{(1)}(1) \right) \tag{30}$$

where we have set $\left.\frac{\partial F_+(q)}{\partial q}\right|_{q=1} = F_+^{(1)}(1)$ according to the general definition of the n-th series coefficient above.
Next we may take derivative of Eq. (27) with respect to q and set $q = 1$ and obtain an equation for $F_+^{(2)}(1)$. We find that it is linearly coupled to $F_+^{(1)}(1)$ as follows:

$$F_+^{(2)}(1) = (1-p_r)^2 \left(M(M-1)\psi_{2,0} + (M-1)\psi_{2,1} F_+^{(1)}(1) + L_2 F_+^{(2)}(1) \right). \tag{31}$$

We may follow the same procedure to obtain equations for the higher derivatives. It is clumsy to do it manually, so we use Mathematica for this. We use symbolic derivatives of Eq. (27) and automatic replacement of terms by the ψ functions using

the *Replace* syntax. The result are the equations for the next two series coefficients.

$$
\begin{aligned}
F_+^{(3)}(1) =&(1-p_r)^3\Big(M(M-1)(M-2)\psi_{3,0}+(M-1)(M-2)\psi_{3,1}F_+^{(1)}(1)\\
&+(M-2)\psi_{3,2}F_+^{(2)}(1)+L_3F_+^{(3)}(1)\Big) \qquad (32)\\
F_+^{(4)}(1) =&(1-p_r)^4\Big(M(M-1)(M-2)(M-3)\psi_{4,0}+(M-1)(M-2)(M-3)\psi_{4,1}F_+^{(1)}(1)\\
&+(M-2)(M-3)\psi_{4,2}F_+^{(2)}(1)+(M-3)\psi_{4,3}F_+^{(3)}(1)+L_4F_+^{(4)}(1)\Big) \qquad (33)
\end{aligned}
$$

Eqs. (30) - (33) relate the four derivates $F_+^{(1)}(1), F_+^{(2)}(1), F_+^{(3)}(1)$ and $F_+^{(4)}(1)$ linearly. So, it is easy to obtain solutions by inverting a 4×4 matrix, using Mathematica. The explicit expressions of the four coefficients are

$$
\begin{aligned}
F_+^{(1)}(1) =&\frac{(1-p_r)M\psi_{1,0}}{1-(1-p_r)L_1} \qquad (34)\\
F_+^{(2)}(1) =&\frac{(1-p_r)^2M(M-1)}{1-(1-p_r)^2L_2}\left[\psi_{2,0}+\frac{2(1-p_r)\psi_{2,1}\psi_{1,0}}{1-(1-p_r)L_1}\right] \qquad (35)\\
F_+^{(3)}(1) =&\frac{(1-p_r)^3M(M-1)(M-2)}{1-(1-p_r)^3L_3}\left[\psi_{3,0}+\frac{3(1-p_r)\psi_{3,1}\psi_{1,0}}{1-(1-p_r)L_1}\right.\\
&\left.+\frac{3(1-p_r)^2\psi_{3,2}\psi_{2,0}}{1-(1-p_r)^2L_2}+\frac{6(1-p_r)^3\psi_{3,2}\psi_{2,1}\psi_{1,0}}{(1-(1-p_r)L_1)(1-(1-p_r)^2L_2)}\right] \qquad (36)\\
F_+^{(4)}(1) =&\frac{(1-p_r)^4M(M-1)(M-2)(M-3)}{1-(1-p_r)^4L_4}\left[\psi_{4,0}+\frac{4(1-p_r)\psi_{4,1}\psi_{1,0}}{1-(1-p_r)L_1}\right.\\
&+\frac{4(1-p_r)^3\psi_{4,3}\psi_{3,0}}{1-(1-p_r)^3L_3}+\frac{6(1-p_r)^2\psi_{4,2}\psi_{2,0}}{1-(1-p_r)^2L_2}+\frac{12(1-p_r)^3\psi_{4,2}\psi_{2,1}\psi_{1,0}}{(1-(1-p_r)L_1)(1-(1-p_r)^2L_2)}\\
&+\frac{12(1-p_r)^4\psi_{4,3}\psi_{3,1}\psi_{1,0}}{(1-(1-p_r)L_1)(1-(1-p_r)^3L_3)}+\frac{12(1-p_r)^5\psi_{4,3}\psi_{3,2}\psi_{2,0}}{(1-(1-p_r)^2L_2)(1-(1-p_r)^3L_3)}\\
&\left.+\frac{24(1-p_r)^6\psi_{4,3}\psi_{3,2}\psi_{2,1}\psi_{1,0}}{(1-(1-p_r)L_1)(1-(1-p_r)^2L_2)(1-(1-p_r)^3L_3)}\right] \qquad (37)
\end{aligned}
$$

In the above expressions, Eqs. (34) - (37), we notice the following patterns. The terms outside the square brackets are of the form $\binom{M}{n}n!\frac{(1-p_r)^n}{1-(1-p_r)^nL_n}$ for the n-th coefficient. Except for the first term, the denominators of the terms inside the square brackets for the n-th coefficient involve factors $(1-(1-p_r)^jL_j)$ with $j\neq n$ or 0. The most crucial fact is that each such term may be associated with a set of integers which are subsets of the set of integers $\{1,2,\cdots,n-1\}$. For example, a subset of $z\leq(n-1)$ positive integer elements is $S_{(n-1)}=(m_z,m_{z-1},\cdots,m_1)=\{m_i\}$ with $i=z,z-1,\cdots,1$, and every $m_i\in\{1,2,\cdots,n-1\}$ and $m_z>m_{z-1}>\cdots m_1$. The power of $(1-p_r)$ in the numerator of each term is equal to $\sum_{i=1}^z m_i$. The subscript of ψ factors are formed by pairs of successive integers drawn from the ordered array of numbers: $n,m_z,m_{z-1},\cdots,m_1,0$. The numeric factors in any numerator can be

absorbed into the ψ factors by introducing the quantities $\phi_{n,m} = \binom{n}{m}\psi_{n,m}$. Putting together all these observations of the patterns, we may write down a general form of $F_+^{(n)}(1)$ as follows:

$$F_+^{(n)}(1) = \binom{M}{n} n! \frac{(1-p_r)^n}{1-(1-p_r)^n L_n} \left[\phi_{n,0} + \sum_{\{S_{(n-1)}\}} \frac{(1-p_r)^{\sum_i m_i} \phi_{n,m_z} \phi_{m_z,m_{z-1}} \cdots \phi_{m_1,0}}{\prod_i (1-(1-p_r)^{m_i} L_{m_i})} \right] \tag{38}$$

where the sum over $\{S_{(n-1)}\}$ runs over all such subsets as $S_{(n-1)}$ mentioned above.

Using Eq. (38) in Eq. (26), we can finally write down the expression of $F_+(q)$ as a series expansion around $q = 1$,

$$\boxed{F_+(q) = \sum_{n=0}^{\infty} (q-1)^n \binom{M}{n} \frac{(1-p_r)^n}{1-(1-p_r)^n L_n} \left[\phi_{n,0} + \sum_{\{S_{(n-1)}\}} \frac{(1-p_r)^{\sum_i m_i} \phi_{n,m_z} \phi_{m_z,m_{z-1}} \cdots \phi_{m_1,0}}{\prod_i (1-(1-p_r)^{m_i} L_{m_i})} \right]} \tag{39}$$

Appendix 4

Relations between the generating functions, and the burst size distribution $B^{ss}(b)$:

Let us denote the probability distribution of having n_- number of docked vesicles before an AP in the steady state by $P_-^{ss}(n_-)$. It is easy to see from similar arguments as in Section , that $P_-^{ss}(n_-)$ will be related to the three distributions: $P_+^{ss}(n_+)$ (to have an initial number), $p(n_-, t_s \mid n_+)$ (for docked vesicles to build up), and $g(t_s)$ (for AP to appear). Thus

$$P_-^{ss}(n_-) = \sum_{n_+} \int_0^{\infty} p(n_-, t_s \mid n_+) P_+^{ss}(n_+) g(t_s) dt_s \tag{40}$$

We define its generating function as

$$F_-(q) = \sum_{n_-=0}^{\infty} q^{n_-} P_-^{ss}(n_-) \tag{41}$$

The ultimate object of our interest, namely the distribution of vesicle burst size b in the steady state, is related to the distribution $P_-^{ss}(n_-)$ as:

$$B^{ss}(b) = \sum_{n_-} P_-^{ss}(n_-) \beta(n_-, p_r, b) \tag{42}$$

Note that the the crucial fact is that we are averaging the well-known binomial distribution now, over the stochastically generated docked vesicle number n_- just prior to an action potential. As we would see, the resultant averaged distribution would be different from the original binomial. The generating function corresponding to $B^{ss}(b)$ is defined as

$$F_b(q) = \sum_{b=0}^{\infty} q^b B^{ss}(b) \tag{43}$$

We have four distributions $p\left(n_-, t_s \mid n_+\right)$, $P_+^{ss}(n_+)$, $P_-^{ss}(n_-)$, and $B^{ss}(b)$ and four corresponding generating functions F, F_+, F_- and F_b, respectively. Of these, we have already calculated F (Eq. (16)) and F_+ (Eq. (39)). We would now proceed to relate the generating functions F_- and F_b to F_+. Once F_b is known explicitly using the expression of F_+, we would then obtain $B^{ss}(b)$ by taking suitable derivatives of $F_b(q)$ with respect to q.
Using Eq. (40) in Eq. (41) we get,

$$\begin{aligned}
F_-(q) &= \sum_{n_-} q^{n_-} \left(\sum_{n_+} \int_0^{\infty} p\left(n_-, t_s \mid n_+\right) P_+^{ss}\left(n_+\right) g(t_s) dt_s \right) \\
&= \int_0^{\infty} g(t_s) dt_s \left\{ \sum_{n_+} P_+^{ss}\left(n_+\right) \sum_{n_-} p\left(n_-, t_s | n_+\right) q^{n_-} \right\} \\
&= \int_0^{\infty} g(t_s) dt_s \left\{ \sum_{n_+} P_+^{ss}\left(n_+\right) F\left(q, t_s \mid n_+\right) \right\}
\end{aligned}$$

In the above we have used the definition of the function F. Substituting the explicit form of $F(q, t_s|n_+)$ from Eq. (16), we have

$$\begin{aligned}
F_-(q) &= \int_0^{\infty} g(t_s) dt_s \left\{ \sum_{n+} P_+^{ss}\left(n_+\right) q^M \left[1 + \frac{1-q}{q} e^{-kt_s}\right]^{M-n_+} \right\} \\
&= \int_0^{\infty} g(t_s) dt_s \left\{ \left[q + (1-q)e^{-kt_s}\right]^M F_+\left(\frac{1}{1 + \frac{1-q}{q} e^{-kt_s}}\right) \right\}
\end{aligned} \tag{44}$$

In the above we have used the definition of F_+.
Substituting $\frac{q-p_r}{1-p_r}$ in place of q in Eq. (25), and noticing $h\left(\frac{q-p_r}{1-p_r}\right) = q$, we get

$$F_+\left(\frac{q-p_r}{1-p_r}\right) = \int_0^{\infty} g(t_s) dt_s \left\{ \left[q + (1-q)e^{-kt_s}\right]^M F_+\left(\frac{1}{1 + \frac{1-q}{q} e^{-kt_s}}\right) \right\} \tag{45}$$

Comparing Eqs. (44) and (45), we immediately get,

$$F_-(q) = F_+\left(\frac{q-p_r}{1-p_r}\right) \tag{46}$$

Substituting Eq. (42) in Eq. (43) with the binomial distribution $\beta(n_-, p_r, b)$ written explicitly, we have

$$\begin{aligned}
F_b(q) &= \sum_b q^b \left(\sum_{n_-} P_-^{ss}(n_-)\binom{n_-}{b} p_r^b (1-p_r)^{n_- - b}\right) \\
&= \sum_{n_-} P_-^{ss}(n_-)\left(qp_r + (1-p_r)\right)^{n_-} \\
&= F_-\left(qp_r + 1 - p_r\right) \\
&= F_+\left(\frac{p_r(q-1)}{1-p_r} + 1\right)
\end{aligned} \tag{47}$$

Here we have used the definition of the function F_-, and the relation of F_+ to F_- from Eq. (46). Using the explicit form of F_+ from Eq. (39), the Eq. (47) gives,

$$F_b(q) = \sum_{n=0}^{\infty}(q-1)^n \binom{M}{n} \frac{p_r^n}{1-(1-p_r)^n L_n}\left[\phi_{n,0} + \sum_{\{S_{(n-1)}\}} \frac{(1-p_r)^{\sum_i m_i}\phi_{n,m_z}\phi_{m_z,m_{z-1}}\cdots\phi_{m_1,0}}{\prod_i (1-(1-p_r)^{m_i}L_{m_i})}\right] \tag{48}$$

We may invert Eq. (43), to obtain the burst size distribution $B^{ss}(b)$ from successive derivatives of $F_b(q)$ as follows:

$$B^{ss}(b) = \frac{1}{b!}\frac{\partial^b F_b(q)}{\partial q^b}\bigg|_{q=0} \tag{49}$$

Note that q is present in $F_b(q)$ only through the factor $(q-1)^n$ in Eq. (48). Using the identity $\frac{\partial^b (q-1)^n}{\partial q^b}\Big|_{q=0} = \frac{n!}{(n-b)!}(-1)^{n-b}$, we obtain our final desired result

$$\boxed{B^{ss}(b) = \sum_{n=0}^{\infty}\binom{n}{b}(-1)^{n-b}\binom{M}{n}\frac{p_r^n}{1-(1-p_r)^n L_n}\left[\phi_{n,0} + \sum_{\{S_{(n-1)}\}} \frac{(1-p_r)^{\sum_i m_i}\phi_{n,m_z}\phi_{m_z,m_{z-1}}\cdots\phi_{m_1,0}}{\prod_i (1-(1-p_r)^{m_i}L_{m_i})}\right]} \tag{50}$$

Appendix 5

The distribution $B^{ss}(b)$ for two special cases of inter AP interval distribution $g(t_s)$

(a) The deterministic case – APs at a fixed frequency $f = 1/T$

Assuming the APs arrive after fixed time duration T, the corresponding distribution $g(t_s) = \delta(t_s - T)$. This is most often the pattern of input spike train used by experimentalists to excite neuronal response at a fixed frequency $f = 1/T$. We may calculate using Eq. (29),

$$\begin{aligned}
\psi_{n,m} &= \int_0^\infty dt_s \delta(t_s - T) e^{-nkt_s}(e^{kt_s} - 1)^{n-m} = e^{-nkT}(e^{kT} - 1)^{n-m}, \\
L_n &= \psi_{n,n} = e^{-nkT}, \\
\psi_{n,m_z}\psi_{m_z,m_{z-1}} \cdots \psi_{m_1,0} &= e^{-nkT}(e^{kT} - 1)^n e^{-kT\sum_{i=1}^z m_i} = (1 - e^{-kT})^n e^{-kT\sum_{i=1}^z m_i}
\end{aligned} \tag{51}$$

Substituting these expressions in the Eq. (50), and recalling $\phi_{n,m} = \binom{n}{m}\psi_{n,m}$, we have

$$\begin{aligned}
B^{ss}(b) &= \sum_{n=0}^{\infty} \binom{n}{b} (-1)^{n-b} \binom{M}{n} \frac{p_r^n}{1 - (1 - p_r)^n L_n} \left[\phi_{n,0} + \sum_{\{S_{(n-1)}\}} \frac{(1 - p_r)^{\sum_i m_i} \phi_{n,m_z}\phi_{m_z,m_{z-1}} \cdots \phi_{m_1,0}}{\prod_i (1 - (1 - p_r)^{m_i} L_{m_i})} \right] \\
&= \sum_{n=0}^{\infty} \binom{n}{b} (-1)^{n-b} \binom{M}{n} \frac{p_r^n}{1 - (e^{-kT}(1 - p_r))^n} (1 - e^{-kT})^n \\
&\qquad \left[1 + \sum_{\{S_{(n-1)}\}} \binom{n}{m_z} \binom{m_z}{m_{z-1}} \cdots \binom{m_2}{m_1} \prod_i \frac{(e^{-kT}(1 - p_r))^{m_i}}{(1 - (e^{-kT}(1 - p_r))^{m_i})} \right]
\end{aligned} \tag{52}$$

It is important to remind that $\{S_{(n-1)}\}$ is the set of all the subsets of the set $\{1, 2, \cdots, n-1\}$. To proceed further, we need to use the following identity (for $|x| < 1$) – for proof see Appendix 6:

$$1 + \sum_{\{S_{(n-1)}\}} \binom{n}{m_z} \binom{m_z}{m_{z-1}} \cdots \binom{m_2}{m_1} \prod_i \frac{x^{m_i}}{(1 - x^{m_i})} = \frac{1 - x^n}{(1 - x)^n} \tag{53}$$

Using the identity (Eq. (53)) in Eq. (52), the expression simplifies to give,

$$
\begin{aligned}
B^{ss}(b) &= \sum_{n=0}^{\infty} \binom{n}{b} (-1)^{n-b} \binom{M}{n} \frac{p_r^n}{1-(e^{-kT}(1-p_r))^n} (1-e^{-kT})^n \frac{1-(e^{-kT}(1-p_r))^n}{(1-e^{-kT}(1-p_r))^n} \\
&= \sum_{n=0}^{\infty} \binom{n}{b} (-1)^{n-b} \binom{M}{n} \frac{p_r^n}{(1-e^{-kT}(1-p_r))^n} (1-e^{-kT})^n \\
&= \sum_{n=0}^{\infty} \binom{n}{b} (-1)^{b} \binom{M}{n} \left(\frac{-p_r(1-e^{-kT})}{1-e^{-kT}(1-p_r)} \right)^n
\end{aligned}
$$

Further using the identity, $\sum_{n=b}^{M} x^n \binom{n}{b} \binom{M}{n} = \binom{M}{b} x^b (x+1)^{M-b}$ we finally get

$$
\boxed{B^{ss}(b) = \binom{M}{b} \left(\frac{(1-e^{-kT})p_r}{1-(1-p_r)e^{-kT}} \right)^b \left(1 - \frac{(1-e^{-kT})p_r}{1-(1-p_r)e^{-kT}} \right)^{M-b} = \beta(M, p_{rb}, b)} \tag{54}
$$

Hence, the steady state burst size distribution for the deterministic $g(t_s)$ is still a binomial distribution, but with the parameters M (maximal docked vesicle number) and an effective release probability p_{rb} (different from p_r) given by:

$$
p_{rb} = \frac{(1-e^{-kT})p_r}{1-(1-p_r)e^{-kT}} \tag{55}
$$

In order to compare the exact distribution (Eq. (54)) with the approximate binomial distribution $\beta(\langle n_- \rangle, p_r, b)$ where $\langle n_- \rangle$ is the mean number of docked vesicles just before the AP spikes, we need to calculate an expression for $\langle n_- \rangle$. It is easy to calculate $\langle n_- \rangle$ from the generating function $F_-(q)$ as $\langle n_- \rangle = \left.\frac{\partial F_-(q)}{\partial q}\right|_{q=1}$.

Taking derivative of Eq. (46) and setting $q = 1$, we get

$$
\left.\frac{\partial F_-(q)}{\partial q}\right|_{q=1} = \left.\frac{\partial F_+(q)}{\partial q}\right|_{q=1} \frac{1}{(1-p_r)} \tag{56}
$$

If we take the derivative of Eq. (39) with respect to q at $q = 1$, only $n = 1$ term in the summation survives. Eq. (56) will become

$$
\left.\frac{\partial F_-(q)}{\partial q}\right|_{q=1} = \frac{M(1-p_r)}{1-(1-p_r)L_1} \phi_{1,0} \frac{1}{(1-p_r)}
$$

Substituting the forms of L_1 and $\phi_{1,0}$ from Eq. (51), we get

$$
\left.\frac{\partial F_-(q)}{\partial q}\right|_{q=1} = \frac{M(1-p_r)}{1-(1-p_r)e^{-kT}} (1-e^{-kT}) \frac{1}{(1-p_r)}
$$

Hence,

$$\boxed{\langle n_- \rangle = \frac{M(1-e^{-kT})}{1-(1-p_r)e^{-kT}} = M\frac{p_{rb}}{p_r}} \tag{57}$$

In the above we have used the expression of p_{rb} from Eq. (55). The Eq. (57) implies that the mean $\langle b \rangle$ of the exact binomial and the approximate binomial are equal, i.e. $Mp_{rb} = \langle n_- \rangle p_r$. But the variance of the exact distribution is $Mp_{rb}(1-p_{rb})$, different from that of the approximate binomial $\langle n_- \rangle p_r(1-p_r)$.

(b) Poisson distributed AP arrival times

APs may arrive at intervals which may be noisy. A simple way to incorporate stochasticity in the input spike train is to assume that they arrive at time intervals which are exponentially distributed with $g(t_s) = f_0 e^{-f_0 t_s}$. Note that the mean as well as characteristic spike interval is $1/f_0$. In this case using Eq. (29),

$$\begin{aligned}
\psi_{n,m} =& \int_0^\infty dt_s g(t_s) e^{-mkt_s}(1-e^{-kt_s})^{n-m} \\
=& \int_0^\infty dt_s f_0 e^{-(mk+f_0)t_s}(1-e^{-kt_s})^{n-m} \\
=& \frac{f_0}{k}\int_0^1 dz z^{\frac{mk+f_0}{k}-1}(1-z)^{n-m} \\
=& \frac{f_0}{k} B\left(m+\frac{f_0}{k}, n-m+1\right) = \frac{f_0}{k}\frac{\Gamma(-m+n+1)\Gamma\left(\frac{f_0}{k}+m\right)}{\Gamma\left(\frac{f_0}{k}+n+1\right)},
\end{aligned} \tag{58}$$

where we have used Beta function $B(a,b) = \Gamma(a)\Gamma(b)/\Gamma(a+b)$, and then

$$L_n = \psi_{n,n} = \frac{f_0}{k}\frac{\Gamma(1)\Gamma\left(\frac{f_0}{k}+n\right)}{\Gamma\left(\frac{f_0}{k}+n+1\right)} = \frac{f_0}{f_0+nk}. \tag{59}$$

Moreover using Eq. (58), we have

$$\begin{aligned}
\phi_{n,m} = \binom{n}{m}\psi_{n,m} =& \binom{n}{m}\frac{f_0}{k}\frac{\Gamma(-m+n+1)\Gamma\left(\frac{f_0}{k}+m\right)}{\Gamma\left(\frac{f_0}{k}+n+1\right)} = \frac{f_0}{k}\frac{\Gamma(n+1)\Gamma\left(\frac{f_0}{k}+m\right)}{\Gamma(m+1)\Gamma\left(\frac{f_0}{k}+n+1\right)} \\
\Rightarrow \phi_{n,m}\phi_{m,l} =& \frac{f_0^2}{k^2}\frac{\Gamma(n+1)\Gamma\left(\frac{f_0}{k}+m\right)}{\Gamma(m+1)\Gamma\left(\frac{f_0}{k}+n+1\right)}\frac{\Gamma(m+1)\Gamma\left(\frac{f_0}{k}+l\right)}{\Gamma(l+1)\Gamma\left(\frac{f_0}{k}+m+1\right)} \\
=& \frac{f_0^2}{k^2}\frac{k\Gamma(n+1)\Gamma\left(\frac{f_0}{k}+l\right)}{\Gamma(l+1)(f_0+km)\Gamma\left(\frac{f_0}{k}+n+1\right)}
\end{aligned} \tag{60}$$

The above Eq. (60) may be extended to get the following product:

$$\phi_{n,m_z}\phi_{m_z,m_{z-1}}\cdots\phi_{m_1,0} = \frac{f_0^{z+1}}{k^{z+1}}\frac{n!\Gamma\left(\frac{f_0}{k}\right)}{\Gamma\left(\frac{f_0}{k}+n+1\right)}\prod_i \frac{k}{f_0+km_i} \tag{61}$$

Substituting Eq. (61) into Eq. (50), we have

$$\begin{aligned}
B^{ss}(b) =& \sum_{n=0}^{\infty}\binom{n}{b}(-1)^{n-b}\binom{M}{n}\frac{p_r^n}{1-(1-p_r)^n L_n}\left[\phi_{n,0} + \sum_{\{S_{(n-1)}\}}\frac{(1-p_r)^{\sum_i m_i}\frac{f_0^{z+1}}{k^{z+1}}\frac{n!\Gamma\left(\frac{f_0}{k}\right)}{\Gamma\left(\frac{f_0}{k}+n+1\right)}\prod_i\frac{k}{f_0+km_i}}{\prod_i(1-(1-p_r)^{m_i}L_{m_i})}\right] \\
=& \sum_{n=0}^{\infty}\binom{n}{b}(-1)^{n-b}\binom{M}{n}\frac{p_r^n}{1-(1-p_r)^n L_n}\frac{n!\Gamma\left(\frac{f_0}{k}\right)}{\Gamma\left(\frac{f_0}{k}+n+1\right)}\frac{f_0}{k}\left[1 + \sum_{\{S_{(n-1)}\}}\frac{(1-p_r)^{\sum_i m_i}\prod_i\frac{f_0}{f_0+km_i}}{\prod_i(1-(1-p_r)^{m_i}L_{m_i})}\right]
\end{aligned}$$

From Eq. (59), substituting $\frac{f_0}{f_0+km_i} = L_{m_i}$, we have

$$B^{ss}(b) = \sum_{n=0}^{\infty}\binom{n}{b}(-1)^{n-b}\binom{M}{n}\frac{p_r^n}{1-(1-p_r)^n L_n}\frac{n!\Gamma\left(\frac{f_0}{k}+1\right)}{\Gamma\left(\frac{f_0}{k}+n+1\right)}\left[1 + \sum_{\{S_{(n-1)}\}}\prod_i\frac{(1-p_r)^{m_i}L_{m_i}}{(1-(1-p_r)^{m_i}L_{m_i})}\right] \tag{62}$$

We may simplify the expression above by using the following identity valid for any arbitrary function f – for proof see Appendix 7:

$$1 + \sum_{\{S_{(n-1)}\}}\prod_i\frac{f(m_i)}{1-f(m_i)} = \frac{1}{\prod_{i=1}^{n-1}(1-f(i))} \tag{63}$$

Using Eq. (63) in Eq. (62), we get

$$B^{ss} = \sum_{n=0}^{\infty}\binom{n}{b}(-1)^{n-b}\binom{M}{n}\frac{p_r^n n!\Gamma\left(\frac{f_0}{k}+1\right)}{(1-(1-p_r)^n L_n)\Gamma\left(\frac{f_0}{k}+n+1\right)}\frac{1}{\prod_{i=1}^{n-1}(1-(1-p_r)^i L_i)}$$

Substituting back $L_i = \frac{f_0}{f_0+ki}$, we have

$$B^{ss} = \sum_{n=0}^{\infty}\binom{n}{b}(-1)^{n-b}\binom{M}{n}\frac{p_r^n n!\Gamma\left(\frac{f_0}{k}+1\right)}{\Gamma\left(\frac{f_0}{k}+n+1\right)}\frac{1}{\prod_{i=1}^{n}\frac{(f_0+ki-(1-p_r)^i f_0)}{f_0+ki}}$$

$$\boxed{B^{ss}(b) = \sum_{n=0}^{\infty}(-1)^{n-b}\binom{n}{b}\binom{M}{n}\frac{n!(kp_r)^n}{\prod_{i=1}^{n}(f_0 + ki - (1-p_r)^i f_0)}} \tag{64}$$

Thus the steady state burst size distribution for the spike intervals drawn from a Poisson processes is not a Binomial, but instead the above distribution in Eq. (64).

Appendix 6

Proof of the identity in Eq. (53):

The identity can be proved using the principle of strong mathematical induction as follows.

We first verify the identity for $n = 1$ and 2 explicitly. For $n = 1$, LHS of Eq. (53) will be simply equal to 1 as the summation term does not contribute anything. The RHS is also equal to 1, so the identity is true for $n = 1$. For $n = 2$, $\{S_{(1)}\} = \{\{1\}\}$. So, the LHS of Eq. (53) will be equal to $1 + \binom{2}{1}\frac{x}{1-x} = \frac{1+x}{1-x} = \frac{1-x^2}{(1-x)^2} = RHS$. Hence, we have verified the identity for $n = 2$ as well.

Let us assume that the identity is true for all integer values of $n \in [1, k]$. We would then show below that it is true for $n = k + 1$. For $n = k + 1$ we have:

$$\begin{aligned} LHS =& 1 + \sum_{\{S_{(k)}\}}\binom{k+1}{m_z}\binom{m_z}{m_{z-1}}\cdots\binom{m_2}{m_1}\prod_i \frac{x^{m_i}}{(1-x^{m_i})} \\ =& 1 + \binom{k+1}{1}\frac{x}{1-x} + \sum_{\substack{\{S_{(k)}\} \\ m_z \neq 1}}\binom{k+1}{m_z}\binom{m_z}{m_{z-1}}\cdots\binom{m_2}{m_1}\prod_i \frac{x^{m_i}}{(1-x^{m_i})} \end{aligned} \tag{65}$$

where in the last step, we have separated out the contribution of $m_z = 1$ in the summation. The crucial step in our proof comes from the idea that the subsets in the set $\{S_{(k)}\}$ (with $m_z \neq 1$) can be clubbed into different groups, such that the largest element in all the subsets in a particular group are equal. There will be $k-1$ such groups as the maximum element m_z can range from 2 to k. With the summing over all such groups explicitly shown, Eq. (65) becomes

$$LHS = 1 + \binom{k+1}{1}\frac{x}{1-x} + \sum_{m_z=2}^{k}\binom{k+1}{m_z}\frac{x^{m_z}}{1-x^{m_z}}\left[\sum_{\{S_{(m_z-1)}\}}\binom{m_z}{m_{z-1}}\cdots\binom{m_2}{m_1}\prod_i \frac{x^{m_i}}{(1-x^{m_i})} + 1\right] \tag{66}$$

Note that 1 is added manually inside the square bracket to take care of the subsets with only one element m_z, as these subsets are not taken into account by the summation term over the subsets $\{S_{(m_z-1)}\}$. The expression inside the square bracket is equal to the LHS of Eq. (53) with $n = m_z$. Note that as positive integer

$m_z \leq k$, by assumption the identity Eq. (53) is true. So, substituting the form of RHS from Eq. (53) into the square bracket of Eq. (66), we have

$$\begin{aligned}
LHS =& 1 + \binom{k+1}{1}\frac{x}{1-x} + \sum_{m_z=2}^{k}\binom{k+1}{m_z}\frac{x^{m_z}}{1-x^{m_z}}\left[\frac{1-x^{m_z}}{(1-x)^{m_z}}\right] \\
=& 1 + \binom{k+1}{1}\frac{x}{1-x} + \sum_{m_z=2}^{k}\binom{k+1}{m_z}\left(\frac{x}{1-x}\right)^{m_z} \\
=& \sum_{m_z=0}^{k}\binom{k+1}{m_z}\left(\frac{x}{1-x}\right)^{m_z} \\
=& \sum_{m_z=0}^{k+1}\binom{k+1}{m_z}\left(\frac{x}{1-x}\right)^{m_z} - \left(\frac{x}{1-x}\right)^{k+1} \\
=& \left(\frac{1}{1-x}\right)^{k+1} - \left(\frac{x}{1-x}\right)^{k+1} \\
=& \frac{1-x^{k+1}}{(1-x)^{k+1}} = RHS
\end{aligned} \tag{67}$$

Hence, we have shown above that the identity is true for $n = k+1$. Since integer $k \geq 2$ is arbitrary, we have proved the identity in Eq. (53) using the method of strong induction.

Appendix 7

Proof of the identity in Eq. (63):

Here is the proof of the identity using the method of mathematical induction:

For $n = 2$, $\{S\}$, the set of all the subsets of $\{1\}$, is simply $\{\{1\}\}$. Hence, the LHS of Eq. (63) will be equal to

$$LHS = 1 + \prod_{\{1\}}\frac{f(m_i)}{1-f(m_i)} = 1 + \frac{f(1)}{1-f(1)} = \frac{1}{1-f(1)} = RHS \tag{68}$$

Let us assume that the identity is true for an arbitrary value of $n = k$. For, $n = k+1$, the set $\{S\}$ of all the subsets of $\{1, 2, 3, \cdots k\}$ can be divided into three disjoint subsets:

(a) the set of all the subsets of $\{1, 2, 3, \cdots k-1\}$.

(b) the set of all the subsets in (a) with an extra element k added to each of the subsets.

(c) $\{\{k\}\}$

Clearly, the contribution of (a) in the summation term in the LHS of Eq. (63)

will be equal to that for $n = k$, that is equal to $1/\prod_{i=1}^{k-1}(1 - f(i)) - 1$. On the other hand, the contribution of (b) will be equal to that of (a) multiplied by an additional factor $\frac{f(k)}{1-f(k)}$. The contribution from (c) will be simply $\frac{f(k)}{1-f(k)}$. Adding all the three contributions,

$$
\begin{aligned}
LHS =& 1 + \left(\frac{1}{\prod_{i=1}^{k-1}(1 - f(i))} - 1 \right) + \left(\frac{1}{\prod_{i=1}^{k-1}(1 - f(i))} - 1 \right) \frac{f(k)}{1 - f(k)} + \frac{f(k)}{1 - f(k)} \\
=& \frac{1}{\prod_{i=1}^{k-1}(1 - f(i))} \left(1 + \frac{f(k)}{1 - f(k)} \right) \\
=& \frac{1}{\prod_{i=1}^{k}(1 - f(i))} = RHS
\end{aligned}
$$

Hence, the identity is true for $n = k+1$. Thus from the principle of mathematical induction, the identity is proved for any integer $n > 1$.